

Fault detection and isolation in the presence of process uncertainties[☆]

Zhengang Han, Weihua Li, Sirish L. Shah*

Department of Chemical and Materials Engineering, University of Alberta, Edmonton, AB, Canada T6G 2G6

Received 27 May 2002; accepted 28 April 2004

Available online 2 July 2004

Abstract

This paper proposes a novel scheme of sensor/actuator fault detection and isolation (FDI) for multivariate dynamic systems in the presence of process uncertainties, including model-plant-mismatch and process disturbances. Given an estimated model that can be biased from the true one, the primary residual vector (PRV), for detecting faults in output sensors, can be made completely insensitive to process uncertainties under certain conditions. For detecting faults in actuators, the PRV can be made almost insensitive to the process uncertainties. Numerical and experimental examples justify the effectiveness of the proposed scheme, where comparison with an existing robust FDI scheme is conducted.

© 2004 Elsevier Ltd. All rights reserved.

Keywords: Fault detection; Fault isolation; Robustness; Uncertainty; Multivariate systems

1. Introduction

Since the 1970s, tremendous research effort has been invested in model-based fault detection and isolation (FDI). So far, survey papers in this area have been published by Willsky (1976), Isermann (1984), Gertler (1988, 1991), and Frank (1990). In addition, several books are also available (Basseville & Nikiforov, 1993; Patton, Frank, & Clark, 1989, 2000; Gertler, 1998). For most recent advances on FDI, reviews have been given by Qin and Li (2001), and Li and Shah (2002).

Early FDI methods assumed the availability of an accurate model of the monitored system. In practice, however, such an assumption can be invalid, because modelling errors, i.e. model-plant-mismatch (MPM), is always present in a complex system. Besides, process disturbances are inevitable in most processes. *Process uncertainties* are referred to MPM and process disturbances herein, and in the sequel throughout this paper this terminology will be always used. Process uncertain-

ties can render most accurate model-based FDI schemes to be non-robust, making them completely unworkable in worst cases.

Recently, robust FDI schemes that enable the detection and isolation of faults in the presence of process uncertainties have drawn increasing research attention. Basically, existing FDI schemes take into consideration of process disturbances and MPM separately. Disturbances decoupling FDI methods include the works done by Frank (1994), and Patton and Chen (1992, 2000). On the other hand, a number of FDI schemes with robustness against the modelling errors have been proposed including the work by Lou, Willsky, and Verghese (1986), Frank and Ding (1994, 1997), Gertler and Kunwer (1995), Chen, Patton, and Zhang (1996), Shen and Hsu (1998), Hamelin and Sauter (2000), Qin and Li (2001), and Li and Shah (2002), in both the time and frequency domains. However, to the best of our knowledge, very few FDI schemes have the capability of simultaneously working in the presence of disturbances plus MPM, unless some restrictive assumptions on the MPM are assumed (Zhong, Ding, Lam, & Wang, 2003; Chen & Patton, 1999).

This paper proposes an online and real time sensor and actuator FDI scheme which takes care of the process disturbances and the MPM simultaneously for a

[☆] An abbreviated version of this paper was published in the Proceedings of the 15th IFAC World Congress, pp. 1887–1892, July 2002, Barcelona, Spain.

*Corresponding author. Tel.: +1-780-492-5162; fax: +1-780-492-2881.

E-mail address: sirish.shah@ualberta.ca (S.L. Shah).

multivariate dynamic system. By extending the well-known Chow–Willsky approach (Chow & Willsky, 1984), a primary residual vector (PRV), which is a fault-accentuated signal, is generated for fault detection. To generate the PRV, one does not need a precise state space model of the considered system. Instead, a roughly estimated model is good enough. To detect and isolate faults in the output sensors only, the PRV can be made perfectly insensitive to the process uncertainties under certain reasonable conditions. To detect and isolate faults in the actuators, the PRV can be made almost insensitive to the process uncertainties.

This paper is organized as follows. Section 2 gives the problem formulation. The design of a PRV for sensor fault detection in the presence of process uncertainties is furnished in Section 3, where a set of structured residual vectors (SRVs) is also generated by transforming the PRV for fault isolation. The detection and isolation of actuator faults are discussed in Section 4. Numerical simulation and experimental case studies are presented in Section 5, where a comparison between the newly proposed robust FDI approach and the original Chow–Willsky approach is included. The paper ends with concluding remarks in Section 6.

2. Problem formulation

2.1. System description

Assume that the normal behavior of a multivariate dynamic process can be represented by the following discrete time linear state space model:

$$\begin{aligned} \mathbf{x}_{k+1} &= \mathbf{A}\mathbf{x}_k + \mathbf{B}\mathbf{u}_k + \mathbf{E}\mathbf{d}_k, \\ \mathbf{y}_k^* &= \mathbf{C}\mathbf{x}_k, \end{aligned} \tag{1}$$

where $\mathbf{u}_k \in \mathfrak{R}^l$ is the process inputs; $\mathbf{y}_k^* \in \mathfrak{R}^m$ is the *fault-free* process outputs; $\mathbf{x}_k \in \mathfrak{R}^n$ is the process state vector; $\mathbf{d}_k \in \mathfrak{R}^q$ represents the unmeasured deterministic process

disturbance vector (Gustafsson & Graebe, 1998), which can be any unknown function of time; $\mathbf{E} \in \mathfrak{R}^{n \times q}$ is a unknown gain matrix of the disturbances; and $\{\mathbf{A}, \mathbf{B}, \mathbf{C}\}$ are system matrices with appropriate dimensions. The process is assumed to be observable.

With the presence of sensor/actuator faults and instrument noises, the inputs to the process and the observed process outputs can be represented by

$$\begin{aligned} \mathbf{u}_k &= \mathbf{u}_k^* + \mathbf{f}_k^u, \\ \mathbf{y}_k &= \mathbf{y}_k^* + \mathbf{f}_k^y + \mathbf{o}_k, \end{aligned} \tag{2}$$

where $\mathbf{y}_k \in \mathfrak{R}^m$ is the measured output vector; $\mathbf{u}_k^* \in \mathfrak{R}^l$ is the *fault-free* input vector to the process; $\mathbf{o}_k \in \mathfrak{R}^m$ is the output measurement noise; $\mathbf{f}_k^u \in \mathfrak{R}^l$ is the actuator fault; and $\mathbf{f}_k^y \in \mathfrak{R}^m$ is the sensor fault. It is assumed that \mathbf{o}_k is a Gaussian-distributed white noise vector with covariance matrix \mathbf{R}_o , and is independent of the initial state \mathbf{x}_0 and the disturbances \mathbf{d}_k .

In the fault-free case, \mathbf{f}_k^u and \mathbf{f}_k^y are null vectors. In the case that some sensors/actuators are faulty, the corresponding elements in \mathbf{f}_k^y and \mathbf{f}_k^u will be non-zero, while the other elements remain zero. For instance, to indicate that the first output sensor is faulty, the first element in \mathbf{f}_k^y is non-zero while other elements are zero.

It is assumed that \mathbf{u}_k^* and \mathbf{y}_k are available, because they are controller outputs and the observed process outputs, respectively. The detailed process setup is displayed in Fig. 1.

2.2. Process uncertainties

In most cases, the true values of the system matrices $\{\mathbf{A}, \mathbf{B}\}$ are never exactly known. However, an estimate $\{\mathbf{A}_o, \mathbf{B}_o\}$ of $\{\mathbf{A}, \mathbf{B}\}$ can be available, and one has

$$\begin{aligned} \mathbf{A} &= \mathbf{A}_o + \delta\mathbf{A}, \\ \mathbf{B} &= \mathbf{B}_o + \delta\mathbf{B}, \end{aligned} \tag{3}$$

where $\{\delta\mathbf{A}, \delta\mathbf{B}\}$ is the error between $\{\mathbf{A}, \mathbf{B}\}$ and $\{\mathbf{A}_o, \mathbf{B}_o\}$, representing the MPM. Assume that \mathbf{C} is

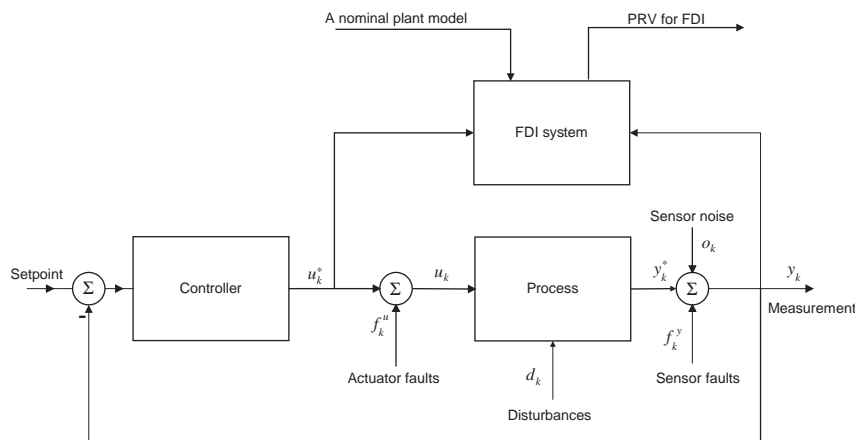


Fig. 1. Schematic diagram of the FDI system.

exactly known, i.e. $\mathbf{C} = \mathbf{C}_o$, because it is the sensor gain matrix. This is a widely accepted assumption in dealing with the issue of MPM (Zhong et al., 2003).

The combination of Eqs. (1)–(3) results in

$$\begin{aligned} \mathbf{x}_{k+1} &= (\mathbf{A}_o + \delta\mathbf{A})\mathbf{x}_k + (\mathbf{B}_o + \delta\mathbf{B})\mathbf{u}_k + \mathbf{E}\mathbf{d}_k \\ &= \mathbf{A}_o\mathbf{x}_k + \mathbf{B}_o\mathbf{u}_k + [\delta\mathbf{A} \ \delta\mathbf{B}] \begin{bmatrix} \mathbf{x}_k \\ \mathbf{u}_k \end{bmatrix} + \mathbf{E}\mathbf{d}_k \\ &= \mathbf{A}_o\mathbf{x}_k + \mathbf{B}_o\mathbf{u}_k^* + \mathbf{e}_k + \mathbf{B}_o\mathbf{f}_k^u, \\ \mathbf{y}_k &= \mathbf{C}_o\mathbf{x}_k + \mathbf{o}_k + \mathbf{f}_k^y, \end{aligned} \quad (4)$$

where $\mathbf{e}_k \equiv \delta\mathbf{A}\mathbf{x}_k + \delta\mathbf{B}\mathbf{u}_k + \mathbf{E}\mathbf{d}_k \in \mathfrak{R}^n$ is the process uncertainty vector accounting for the effects of the MPM and process disturbances. The following remarks can be made for Eq. (4).

Remark 2.1. The gain matrix that links the process uncertainty vector \mathbf{e}_k and the state vector \mathbf{x}_{k+1} is an $n \times n$ identity matrix \mathbf{I}_n . With such a constant matrix, decoupling \mathbf{e}_k from the PRV is feasible, provided that certain conditions are met.

Remark 2.2. In the presence of actuator faults, $\mathbf{e}_k = \delta\mathbf{A}\mathbf{x}_k + \delta\mathbf{B}\mathbf{u}_k^* + \delta\mathbf{B}\mathbf{f}_k^u + \mathbf{E}\mathbf{d}_k$. In this case, $\mathbf{e}_k = \mathbf{e}_k^* + \mathbf{e}_k^f$, where $\mathbf{e}_k^* = \delta\mathbf{A}\mathbf{x}_k + \delta\mathbf{B}\mathbf{u}_k^* + \mathbf{E}\mathbf{d}_k$ is the fault-free part, while $\mathbf{e}_k^f = \delta\mathbf{B}\mathbf{f}_k^u$ is the fault-related part.

Remark 2.3. Due to the assumption made on \mathbf{d}_k (Gustafsson & Graebe, 1998), it can be shown that \mathbf{e}_k^* is a deterministic vector, if the initial state, i.e. \mathbf{x}_\emptyset , is not random. In addition, it is assumed that \mathbf{e}_k^* is bounded, e.g. $\|\mathbf{e}_k^*\| \leq L_m$, where $\|\cdot\|$ stands for the L_2 -norm. This means that physically, process uncertainties only affect the process dynamics to some extent. Note that \mathbf{e}_k^* consists of three terms, and $\|\mathbf{e}_k^*\| = \|\delta\mathbf{A}\mathbf{x}_k + \delta\mathbf{B}\mathbf{u}_k^* + \mathbf{E}\mathbf{d}_k\| \leq \|\delta\mathbf{A}\mathbf{x}_k\| + \|\delta\mathbf{B}\mathbf{u}_k^*\| + \|\mathbf{E}\mathbf{d}_k\|$. If we further assume that each term has less energy acting on the system than the known input term $\|\mathbf{B}_o\mathbf{u}_k^*\|$, then we can determine L_m to be equal to $\max_{k \in [1, \dots]} \{3\|\mathbf{B}_o\mathbf{u}_k^*\|\}$.

2.3. Problem of FDI in the presence of process uncertainties

With Eq. (4), the problem of FDI for the system of Eq. (1) can be stated as follows:

- (1) From a set of training data, obtain an estimate $\{\mathbf{A}_o, \mathbf{B}_o, \mathbf{C}_o\}$ of the system matrices. This can be done by using any existing algorithm of subspace method of identification (SMI), e.g. the *N4SID* function in *Matlab*[®].
- (2) In terms of the estimated system matrices, generate a PRV that is perfectly or almost perfectly independent of the process uncertainty vector \mathbf{e}_k for fault detection.

- (3) By manipulating the PRV algebraically, pinpoint the faulty sensors and/or actuators.

3. Robust sensor FDI

This section is devoted to the detection and isolation of faults in the output sensors of the considered system. To achieve this goal, one has to generate a PRV. The key to the PRV generation is the derivation of a stacked equation.

3.1. Derivation of the stacked equation for PRV generation

Starting from the time instant $k - s$, after performing a series of recursions on Eq. (4), one arrives at

$$\begin{aligned} \mathbf{x}_{k-s+i} &= \mathbf{A}_o^i \mathbf{x}_{k-s} + \sum_{\tau=k-s}^{k-s+i-1} \mathbf{A}_o^{k-s+i-1-\tau} [\mathbf{B}_o \mathbf{u}_\tau^* + \mathbf{e}_\tau + \mathbf{B}_o \mathbf{f}_\tau^u] \\ \text{and} \\ \mathbf{y}_{k-s+i} &= \mathbf{C}_o \mathbf{A}_o^i \mathbf{x}_{k-s} + \mathbf{C}_o \sum_{\tau=k-s}^{k-s+i-1} \mathbf{A}_o^{k-s+i-1-\tau} \\ &\quad \times [\mathbf{B}_o \mathbf{u}_\tau^* + \mathbf{e}_\tau + \mathbf{B}_o \mathbf{f}_\tau^u] + \mathbf{o}_{k-s+i} + \mathbf{f}_{k-s+i}^y, \end{aligned} \quad (5)$$

where $i \in [1, s]$, s is the order of the parity space (Chow & Willsky, 1984), and \mathbf{x}_{k-s} is the state vector at time instant $k - s$. In the following text, $s = n$ is selected.

By stacking Eq. (5), it follows that

$$\begin{aligned} \mathbf{y}_{s,k} - \mathbf{H}_s^o \mathbf{u}_{s-1,k-1}^* &= \mathbf{\Gamma}_s^o \mathbf{x}_{k-s} + \mathbf{f}_{s,k}^y + \mathbf{H}_s^o \mathbf{f}_{s-1,k-1}^u \\ &\quad + \mathbf{G}_s^o \mathbf{e}_{s-1,k-1} + \mathbf{o}_{s,k} \\ &= [\mathbf{\Gamma}_s^o \mid \mathbf{G}_s^o] \begin{bmatrix} \mathbf{x}_{k-s} \\ \mathbf{e}_{s-1,k-1} \end{bmatrix} + \mathbf{f}_{s,k}^y \\ &\quad + \mathbf{H}_s^o \mathbf{f}_{s-1,k-1}^u + \mathbf{o}_{s,k}, \end{aligned} \quad (6)$$

where, $\mathbf{y}_{s,k} = [\mathbf{y}'_{k-s} \ \dots \ \mathbf{y}'_k] \in \mathfrak{R}^{m_s}$ is the stacked output vector,

$$\mathbf{\Gamma}_s^o = [(\mathbf{C}_o)^\circ \ (\mathbf{C}_o \mathbf{A}_o)^\circ \ \dots \ (\mathbf{C}_o \mathbf{A}_o^{s-1})^\circ] \in \mathfrak{R}^{m_s \times n}$$

is the extended observability matrix; and

$$\mathbf{H}_s^o = \begin{bmatrix} \mathbf{0} & \mathbf{0} & \dots & \mathbf{0} \\ \mathbf{C}_o \mathbf{B}_o & \mathbf{0} & \dots & \mathbf{0} \\ \vdots & \vdots & \ddots & \vdots \\ \mathbf{C}_o \mathbf{A}_o^{s-1} \mathbf{B}_o & \mathbf{C}_o \mathbf{A}_o^{s-2} \mathbf{B}_o & \dots & \mathbf{C}_o \mathbf{B}_o \end{bmatrix} \in \mathfrak{R}^{m_s \times ls}$$

and

$$\mathbf{G}_s^o = \begin{bmatrix} \mathbf{0} & \mathbf{0} & \dots & \mathbf{0} \\ \mathbf{C}_o & \mathbf{0} & \dots & \mathbf{0} \\ \vdots & \vdots & \ddots & \vdots \\ \mathbf{C}_o \mathbf{A}_o^{s-1} & \mathbf{C}_o \mathbf{A}_o^{s-2} & \dots & \mathbf{C}_o \end{bmatrix} \in \mathfrak{R}^{m_s \times ns}$$

are two lower triangular block Toeplitz matrices with $m_s = m(s + 1)$. In addition, $\mathbf{u}_{s-1,k-1}^* \in \mathfrak{R}^{ls}$, $\mathbf{f}_{s,k}^y \in \mathfrak{R}^{m_s}$, $\mathbf{f}_{s-1,k-1}^u \in \mathfrak{R}^{ls}$, $\mathbf{e}_{s-1,k-1} \in \mathfrak{R}^{ns}$ and $\mathbf{o}_{s,k} \in \mathfrak{R}^{m_s}$ are also stacked vectors similar to $\mathbf{y}_{s,k}$. Note that in Eq. (6), the

stacked uncertainty vector $\mathbf{e}_{s-1,k-1}$ and the unknown state vector \mathbf{x}_{k-s} have gain matrices \mathbf{G}_s° and \mathbf{I}_s° , respectively.

3.2. Sensor fault detection

Since in this section only the detection and isolation of faults in the output sensors is considered, Eq. (6) can be simplified into

$$\mathbf{y}_{s,k} - \mathbf{H}_s^\circ \mathbf{u}_{s-1,k-1}^* = \Psi_s^\circ \begin{bmatrix} \mathbf{x}_{k-s} \\ \mathbf{e}_{s-1,k-1} \end{bmatrix} + \mathbf{f}_{s,k}^y + \mathbf{o}_{s,k}, \quad (7)$$

where $\Psi_s^\circ \equiv [\mathbf{I}_s^\circ | \mathbf{G}_s^\circ] \in \mathfrak{R}^{m_s \times (n+ns)}$. Select a transformation matrix \mathbf{W}_\circ , which is located in the *left null space* of Ψ_s° , i.e. $\mathbf{W}_\circ \Psi_s^\circ \equiv \mathbf{0}$, and has maximized covariance with the gain matrix \mathbf{I}_{m_s} of $\mathbf{f}_{s,k}^y$. Note that similarly \mathbf{I}_{m_s} is an $m_s \times m_s$ identity matrix. According to the algorithm proposed by Li and Shah (2002), the solution to \mathbf{W}_\circ is $\mathbf{W}'_\circ =$ eigenvectors associated with the non-zero

$$\text{eigenvalues of matrix } (\Psi_s^\circ)^\perp, \quad (8)$$

where $(\Psi_s^\circ)^\perp = \mathbf{I}_{m_s} - \Psi_s^\circ (\Psi_s^\circ)^\dagger$, and $(\Psi_s^\circ)^\dagger$ stands for the Moore–Penrose pseudo inverse (Golub & Van Loan, 1996).

Assume that Ψ_s° is of rank $ns + n$. This is the worst case with respect to uncertainty decoupling from the PRV. As a result, $(\Psi_s^\circ)^\perp$ has at least $m_s - ns - n$ non-zero eigenvalues, and \mathbf{W}'_\circ are the associated $m_s - ns - n$ eigenvectors.

Pre-multiplying both sides of Eq. (7) by \mathbf{W}_\circ leads to

$$\begin{aligned} \boldsymbol{\varepsilon}_{s,k} &\equiv \mathbf{W}_\circ [\mathbf{I}_{m_s} | -\mathbf{H}_s^\circ] \begin{bmatrix} \mathbf{y}_{s,k} \\ \mathbf{u}_{s-1,k-1}^* \end{bmatrix} \\ &= \mathbf{W}_\circ \mathbf{f}_{s,k}^y + \mathbf{W}_\circ \mathbf{o}_{s,k} \in \mathfrak{R}^{m_s - ns - n}, \end{aligned} \quad (9)$$

where $\mathbf{W}_\circ \Psi_s^\circ \equiv \mathbf{0}$ has been employed. As a result, both the unknown state vector \mathbf{x}_{k-s} and the process uncertainty vector $\mathbf{e}_{s-1,k-1}$ have been removed from $\boldsymbol{\varepsilon}_{s,k}$. Define $\boldsymbol{\varepsilon}_{s,k}$ as a PRV for fault detection and have the following remarks:

Remark 3.1. On the right-hand side of Eq. (9), the first line is the computational form, and $\mathbf{W}_\circ [\mathbf{I}_{m_s} | -\mathbf{H}_s^\circ]$ is referred to as the *PRV model*. In addition, the second line is the internal form showing how the output sensor faults affect the PRV.

Remark 3.2. Without fault, $\boldsymbol{\varepsilon}_{s,k} = \boldsymbol{\varepsilon}_{s,k}^* = \mathbf{W}_\circ \mathbf{o}_{s,k}$, which is a moving average (MA) of measurement noise \mathbf{o}_k . From the distribution of \mathbf{o}_k , it can be concluded that $\boldsymbol{\varepsilon}_{s,k}^*$ is also a zero-mean Gaussian-distributed random vector (Johnson & Wichern, 1998) with covariance matrix $\mathbf{R}_{s,e} = \mathbf{W}_\circ \mathbf{R}_{s,o} \mathbf{W}'_\circ$, i.e. $\boldsymbol{\varepsilon}_{s,k}^* \sim \mathcal{N}(\mathbf{0}, \mathbf{R}_{s,e})$, where $\mathbf{R}_{s,o} = \mathbf{I}_{s+1} \otimes \mathbf{R}_o \in \mathfrak{R}^{m_s \times m_s}$ is the covariance matrix of $\mathbf{o}_{s,k}$ and \otimes stands for the kronecker tensor product.

Remark 3.3. With the occurrence of faults,

$$\boldsymbol{\varepsilon}_{s,k} = \boldsymbol{\varepsilon}_{s,k}^f + \boldsymbol{\varepsilon}_{s,k}^*, \quad (10)$$

where $\boldsymbol{\varepsilon}_{s,k}^f = \mathbf{W}_\circ \mathbf{f}_{s,k}^y$ is the fault-contribution term. In this case, $\boldsymbol{\varepsilon}_{s,k}^f$ is a Gaussian-distributed random vector with mean $\boldsymbol{\varepsilon}_{s,k}^f$ and covariance $\mathbf{R}_{s,e}$, i.e. $\boldsymbol{\varepsilon}_{s,k} \sim \mathcal{N}(\boldsymbol{\varepsilon}_{s,k}^f, \mathbf{R}_{s,e})$. Suppose that $\mathbf{W}_\circ \mathbf{f}_{s,k}^y \neq \mathbf{0}$. Consequently, fault detection can be carried out by simply checking if the mean of $\boldsymbol{\varepsilon}_{s,k}$ has deviated from zero.

One can define the following scalar squared weighted residual (SWR):

$$\eta_{s,k} = \boldsymbol{\varepsilon}_{s,k}' \mathbf{R}_{s,e}^{-1} \boldsymbol{\varepsilon}_{s,k} \quad (11)$$

as the fault detection index. In the fault-free case, $\boldsymbol{\varepsilon}_{s,k} = \boldsymbol{\varepsilon}_{s,k}^*$, correspondingly $\eta_{s,k}$ follows a central chi-square distribution with $m_s - ns - n$ degrees of freedom (Johnson & Wichern, 1998), i.e. $\eta_{s,k} \sim \chi^2(m_s - ns - n)$. However, if any sensor is faulty, $\eta_{s,k}$ will no longer follow the central chi-square distribution (Basseville, 1998). Therefore, fault detection can be carried out by comparing $\eta_{s,k}$ against a pre-determined threshold $\chi_\alpha^2(m_s - ns - n)$, where α is a selected level of significance, e.g. $\alpha = 5\%$. While $\eta_{s,k} < \chi_\alpha^2(m_s - ns - n)$ indicates that no fault occurs in sensors, $\eta_{s,k} \geq \chi_\alpha^2(m_s - ns - n)$ implies that some sensors are faulty.

3.3. Sensor fault isolation

Once faults have been detected, one has to identify the faulty sensors. To reach this objective, the PRV must be transformed into a set of SRVs, where one SRV is made insensitive to a subset of sensor faults but most sensitive to the other sensor faults.

In the considered system, there are m sensors. Generally, to isolate faults in all m sensors, m SRVs should be generated. Without loss of generality, the case of isolating a *single* sensor fault at each time is considered. Correspondingly, choose an incidence matrix given in Table 1 to characterize the SRVs' sensitivity and insensitivity to different faults. The selection of incidence matrix is not unique. For detailed discussion, one can refer to Gertler and Singer (1985, 1990), and Li and Shah (2002).

Denote

$$\mathbf{W}_{\circ,i} = [\mathbf{W}_\circ(:,i) \ \mathbf{W}_\circ(:,i+m) \ \cdots \ \mathbf{W}_\circ(:,i+ms)] \quad \forall i = [1, m],$$

where $\mathbf{W}_\circ(:,j)$ for $1 \leq j \leq m_s$ is the j th column of \mathbf{W}_\circ . Note that the stacked fault vector is $\mathbf{f}_{s,k}^y = [(\mathbf{f}_{k-s}^y)' \ (\mathbf{f}_{k-s+1}^y)' \ \cdots \ (\mathbf{f}_k^y)']'$, and $\mathbf{W}_{\circ,i}$ contains the columns in \mathbf{W}_\circ associated with the stacked i th sensor fault $[0 \ \cdots \ 0 \ f_{k-s,i}^y \ 0 \ \cdots \ 0 \ f_{k-1,i}^y \ 0 \ \cdots \ 0 \ f_{k,i}^y \ 0 \ \cdots \ 0]'$,

where $f_{k-s,i}^y$ is the i th element of \mathbf{f}_{k-s}^y .

In the incidence matrix given in Table 1, m SRVs are generated, where the i th SRV, $\mathbf{r}_{s,k}^i$, is insensitive to the afore-mentioned i th stacked sensor fault, but is most

Table 1
Incidence matrix to characterize the isolation logic of sensor faults

| | $f_{k,1}^y$ | $f_{k,2}^y$ | $f_{k,3}^y$ | ... | $f_{k,m}^y$ |
|----------------------|-------------|-------------|-------------|----------|-------------|
| $\mathbf{r}_{s,k}^1$ | 0 | 1 | 1 | ... | 1 |
| $\mathbf{r}_{s,k}^2$ | 1 | 0 | 1 | ... | 1 |
| $\mathbf{r}_{s,k}^3$ | 1 | 1 | 0 | ... | 1 |
| $\mathbf{r}_{s,k}^4$ | 1 | 1 | 1 | ... | 1 |
| \vdots | \vdots | \vdots | \vdots | \ddots | \vdots |
| $\mathbf{r}_{s,k}^m$ | 1 | 1 | 1 | ... | 0 |

sensitive to all other faults. Furthermore, a “0”/“1” corresponding to one SRV and one fault in the incidence matrix indicates that the SRV is designed to be insensitive/most sensitive to the fault. With such an incidence matrix, each fault can be isolated by observing different behavior of the SRVs. For example, if $\mathbf{r}_{s,k}^1$ is unaffected while all the other SRVs: $\mathbf{r}_{s,k}^2$ to $\mathbf{r}_{s,k}^m$ are affected by a fault, it can be concluded that a fault has occurred in the first sensor.

Mathematically, the i th SRV is calculated by multiplying a transformation matrix \mathbf{W}_i on both sides of Eq. (9)

$$\mathbf{r}_{s,k}^i = \mathbf{W}_i \mathbf{e}_{s,k} = \mathbf{W}_i \mathbf{W}_o \mathbf{f}_{s,k}^y + \mathbf{W}_i \mathbf{W}_o \mathbf{o}_{s,k}. \quad (12)$$

To ensure that $\mathbf{r}_{s,k}^i$ is insensitive to the i th sensor, \mathbf{W}_i should be orthogonal to $\mathbf{W}_{o,i}$, i.e. $\mathbf{W}_i \mathbf{W}_{o,i} = \mathbf{0}$, $\forall i = [1, m]$.

In accordance with the algorithm given by Li and Shah (2002), one can calculate \mathbf{W}_i as follows:

$$\mathbf{W}_i' = \text{eigenvectors associated with the non-zero eigenvalues of matrix } \mathbf{W}_{o,i}^\perp \mathbf{W}_o \mathbf{W}_o', \quad (13)$$

where $\mathbf{W}_{o,i}^\perp = \mathbf{I}_{m_s - ns - n} - \mathbf{W}_{o,i} \mathbf{W}_{o,i}^\dagger$. As a result, $\mathbf{r}_{s,k}^i$ has $m_s - ns - n - (s + 1)$ independent rows. Using $\mathbf{r}_{s,k}^i$, one can similarly calculate the isolation indices $\eta_{s,k}^i = (\mathbf{r}_{s,k}^i)' (\mathbf{R}_{s,\varepsilon}^i)^{-1} \mathbf{r}_{s,k}^i$, $\forall i = [1, m]$, where $\mathbf{R}_{s,\varepsilon}^i = \mathbf{W}_i \mathbf{R}_{s,\varepsilon} \mathbf{W}_i'$ is the covariance matrix of $\mathbf{r}_{s,k}^i$. With respect to the sensitivity or insensitivity to a fault, $\eta_{s,k}^i$ is equivalent to $\mathbf{r}_{s,k}^i$.

In accordance with the similar isolation logic defined in Table 1, if

$$\eta_{s,k}^i \leq \chi_\alpha^2 (m_s - ns - n - s - 1), \quad i \in [1, m]$$

and

$$\eta_{s,k}^j \geq \chi_\alpha^2 (m_s - ns - n - s - 1) \quad \forall j \in [1, m] \cap \{j \neq i\},$$

then it can be concluded that the i th output sensor is faulty.

3.4. Condition for perfectly decoupling the uncertainty vector

As shown in Eq. (9), the PRV is $(m_s - ns - n)$ -dimensional. To make the PRV perfectly uncorrelated with any process uncertainties, $m_s - ns - n = (m - n)(s + 1) > 0$, i.e. $m - n > 0$, must be satisfied for fault detection. Furthermore, to leave enough degrees of freedom for the design of the SRVs for fault isolation, a more restrictive condition should also be met. For example, to isolate a single fault at each time in accordance with the isolation logic summarized in Table 1, $m_s - ns - n - (s + 1) = (m - n - 1)(s + 1) > 0$, i.e. $m - n - 1 > 0$, must be guaranteed.

However, $m - n - 1 > 0$ is a reasonable condition. For examples, since most industrial processes have redundant and/or duplicate sensors for critical variables, usually the number of sensors, i.e. m , is expected to be greater than the order of the model, i.e. n , in a chemical process.

4. Robust actuator FDI

In the case that there are faults in the actuators of a considered system, perfect decoupling of process uncertainties from the PRV is not achievable. This will be analyzed later. Nevertheless, decoupling the principal components of the uncertainties from the PRV is still feasible.

4.1. Difficulty in completely decoupling the uncertainties from the PRV

For simplicity, only the actuator faults are considered, neglecting the sensor faults. Consequently, Eq. (6) is reduced to

$$\mathbf{y}_{s,k} - \mathbf{H}_s^\circ \mathbf{u}_{s-1,k-1}^* = [\Gamma_s^\circ \mid \mathbf{G}_s^\circ] \begin{bmatrix} \mathbf{x}_{k-s} \\ \mathbf{e}_{s-1,k-1} \end{bmatrix} + \mathbf{H}_s^\circ \mathbf{f}_{s-1,k-1}^u + \mathbf{o}_{s,k}, \quad (14)$$

where the fault gain matrix is \mathbf{H}_s° .

Note that $\mathbf{H}_s^\circ = \mathbf{G}_s^\circ (\mathbf{I}_s \otimes \mathbf{B}_o)$, where \mathbf{I}_s is an $s \times s$ identity matrix. If selecting a matrix \mathbf{W}_o that is orthogonal to $[\Gamma_s^\circ \mid \mathbf{G}_s^\circ]$, i.e. $\mathbf{W}_o [\Gamma_s^\circ \mid \mathbf{G}_s^\circ] = \mathbf{0}$, and pre-multiply Eq. (14) by \mathbf{W}_o , the resulting PRV is as follows:

$$\mathbf{e}_{s,k} = \mathbf{W}_o (\mathbf{y}_{s,k} - \mathbf{H}_s^\circ \mathbf{u}_{s-1,k-1}^*) = \mathbf{W}_o \mathbf{o}_{s,k}. \quad (15)$$

In the preceding equation, besides \mathbf{x}_{k-s} and $\mathbf{e}_{s-1,k-1}$, the fault-contribution term $\mathbf{H}_s^\circ \mathbf{f}_{s-1,k-1}^u$ is also removed, indicating that the PRV is insensitive to both the faults and the process uncertainties. Therefore, no actuator fault is detectable if the uncertainties are perfectly decoupled.

4.2. Generation of PRV for actuator FDI

To detect and further isolate the actuator faults, one has to compromise in the design of the PRV, e.g., making the PRV insensitive to the principal components of the process uncertainties but sensitive to the faults as much as possible.

Performing the singular value decomposition (SVD) (Golub & Van Loan, 1996) on matrix \mathbf{G}_s° results in

$$\mathbf{G}_s^\circ = \mathbf{U}_G \mathbf{S}_G \mathbf{V}_G', \quad (16)$$

where $\mathbf{S}_G \in \mathfrak{R}^{ns \times ns}$ is a diagonal matrix with singular values in decreasing order, and $\mathbf{U}_G \in \mathfrak{R}^{ms \times ns}$ and $\mathbf{V}_G \in \mathfrak{R}^{ns \times ns}$ contain the left and right singular vectors, respectively.

Eq. (16) can be further split into two parts, e.g.,

$$\mathbf{G}_s^\circ = \mathbf{U}_G \mathbf{S}_G \mathbf{V}_G' = \mathbf{U}_{G,1} \mathbf{S}_{G,1} \mathbf{V}_{G,1}' + \mathbf{U}_{G,2} \mathbf{S}_{G,2} \mathbf{V}_{G,2}', \quad (17)$$

where $\mathbf{S}_{G,1} \in \mathfrak{R}^{n_0 \times n_0}$ is the main submatrix of \mathbf{S}_G containing n_0 principal singular values with $1 \leq n_0 < ns$, and $\{\mathbf{U}_{G,1}, \mathbf{V}_{G,1}\}$ are the associated principal left and right singular vectors in $\{\mathbf{U}_G, \mathbf{V}_G\}$. In addition, $\mathbf{S}_{G,2} \in \mathfrak{R}^{(ns-n_0) \times (ns-n_0)}$ is the remaining submatrix of \mathbf{S}_G , and $\{\mathbf{U}_{G,2}, \mathbf{V}_{G,2}\}$ are the associated remaining columns in $\{\mathbf{U}_G, \mathbf{V}_G\}$. The choice of n_0 will be discussed later.

Substituting Eq. (17) into Eq. (14) gives

$$\begin{aligned} \mathbf{y}_{s,k} - \mathbf{H}_s^\circ \mathbf{u}_{s,k}^* &= \mathbf{\Gamma}_s^\circ \mathbf{x}_{k-s} + \mathbf{U}_{G,1} \mathbf{S}_{G,1} \mathbf{V}_{G,1}' \mathbf{e}_{s-1,k-1} \\ &\quad + \mathbf{U}_{G,2} \mathbf{S}_{G,2} \mathbf{V}_{G,2}' \mathbf{e}_{s-1,k-1} \\ &\quad + \mathbf{H}_s^\circ \mathbf{f}_{s-1,k-1}^u + \mathbf{o}_{s,k}. \end{aligned} \quad (18)$$

Denote $\mathbf{\Psi}_{s,1}^\circ = [\mathbf{\Gamma}_s^\circ \mid \mathbf{U}_{G,1}] \in \mathfrak{R}^{ms \times (n+n_0)}$. Following the method shown in Section 3, design a \mathbf{W}_\circ such that it is orthogonal to $\mathbf{\Psi}_{s,1}^\circ$, i.e. $\mathbf{W}_\circ \mathbf{\Psi}_{s,1}^\circ \equiv \mathbf{0}$, while having a maximized covariance with \mathbf{H}_s° . Mathematically,

\mathbf{W}_\circ' = eigenvectors associated with the non-zero eigenvalues of matrix $(\mathbf{\Psi}_{s,1}^\circ)^\perp \mathbf{H}_s^\circ (\mathbf{H}_s^\circ)'$, (19)

where similarly $(\mathbf{\Psi}_{s,1}^\circ)^\perp = \mathbf{I}_{ms} - \mathbf{\Psi}_{s,1}^\circ (\mathbf{\Psi}_{s,1}^\circ)^\dagger$. As a consequence, the PRV is

$$\begin{aligned} \mathbf{e}_{s,k} &= \mathbf{W}_\circ \mathbf{H}_s^\circ \mathbf{f}_{s-1,k-1}^u + \mathbf{W}_\circ \mathbf{U}_{G,2} \mathbf{S}_{G,2} \mathbf{V}_{G,2}' \mathbf{e}_{s-1,k-1} \\ &\quad + \mathbf{W}_\circ \mathbf{o}_{s,k} \in \mathfrak{R}^{ms-n_0-n}, \end{aligned} \quad (20)$$

where from Remark 2.2, $\mathbf{e}_{s-1,k-1} = \mathbf{e}_{s-1,k-1}^* + (\mathbf{I}_s \otimes \delta \mathbf{B}) \mathbf{f}_{s-1,k-1}^u$, and $\mathbf{e}_{s-1,k-1}^*$ is stacked from \mathbf{e}_k^* .

The PRV can be further decomposed as

$$\mathbf{e}_{s,k} = \mathbf{e}_{s,k}^* + \mathbf{e}_{s,k}^f, \quad (21)$$

where $\mathbf{e}_{s,k}^f = [\mathbf{W}_\circ \mathbf{H}_s^\circ + \mathbf{M}(\mathbf{I}_s \otimes \delta \mathbf{B})] \mathbf{f}_{s-1,k-1}^u$ is the fault term, and $\mathbf{e}_{s,k}^* = \mathbf{W}_\circ \mathbf{o}_{s,k} + \mathbf{M} \mathbf{e}_{s-1,k-1}^*$ is the fault-free term with $\mathbf{M} = \mathbf{W}_\circ \mathbf{U}_{G,2} \mathbf{S}_{G,2} \mathbf{V}_{G,2}'$.

As mentioned in Remark 2.3, \mathbf{e}_k^* is deterministic. As a result, the stacked vector $\mathbf{e}_{s-1,k-1}^*$ is also deterministic. Due to the existence of the process uncertainty-related term $\mathbf{M} \mathbf{e}_{s-1,k-1}^*$, the fault-free term $\mathbf{e}_{s,k}^*$ in the PRV is no longer zero mean. Instead, its mean is $E\{\mathbf{e}_{s,k}^*\} =$

$\mathbf{M} \mathbf{e}_{s-1,k-1}^*$, where $E\{\cdot\}$ denotes the expectation of the argument.

In the fault-free case, the fault detection index $\eta_{s,k} = \mathbf{e}_{s,k}' \mathbf{R}_{s,e}^{-1} \mathbf{e}_{s,k}$ is reduced to $\eta_{s,k}^* = (\mathbf{e}_{s,k}^*)' \mathbf{R}_{s,e}^{-1} \mathbf{e}_{s,k}^*$, which follows a non-central chi-square distribution with $m_s - n - n_0$ degrees of freedom and non-centrality parameter $\|\mathbf{M} \mathbf{e}_{s-1,k-1}^*\|^2$, i.e. $\eta_{s,k}^* \sim \chi^2(m_s - n - n_0, \|\mathbf{M} \mathbf{e}_{s-1,k-1}^*\|^2)$ (Proakis, 1989).

Denote the maximum eigenvalue of $\mathbf{M}'\mathbf{M}$ by λ_{max}^M . From the Courant-Fischer minimax theorem (Golub & Van Loan, 1996), it can be inferred that

$$\|\mathbf{M} \mathbf{e}_{s-1,k-1}^*\|^2 \leq \|\mathbf{e}_{s-1,k-1}^*\|^2 \lambda_{max}^M.$$

Furthermore, it follows from $\|\mathbf{e}_k^*\| \leq L_m$ that $\|\mathbf{e}_{s-1,k-1}^*\|^2 \leq s^2 L_m^2$, indicating that the upper limit of the non-centrality parameter is $s^2 L_m^2 \lambda_{max}^M$. Therefore, with a selected level of significance α , one can choose $\chi_\alpha^2(m_s - n - n_0, s^2 L_m^2 \lambda_{max}^M)$ as the threshold for $\eta_{s,k}$. Then fault detection can be similarly carried out by comparing $\eta_{s,k}$ against the threshold.

Eventually, to isolate faults, one can transform the PRV into a set of SRVs as one has done in Section 3.3. One can also use the isolation logic in Table 1 to determine the sensitivity and insensitivity of the SRVs with respect to a fault. Moreover, using the SRVs, one can construct the fault isolation indices $\eta_{s,k}^i$, $i = 1, \dots, l$. After determining the thresholds for each $\eta_{s,k}^i$, fault isolation can be similarly performed as in Section 3.3.

4.3. Conditions for decoupling the principal components of uncertainties from the PRV and fault detectability

4.3.1. Choice of n_0

Denote $\text{Rank}\{(\mathbf{\Psi}_{s,1}^\circ)^\perp \mathbf{H}_s^\circ (\mathbf{H}_s^\circ)'\} = p$, where $\text{Rank}\{\cdot\}$ represents the rank of a matrix. From Eqs. (19) and (20), it can be concluded that the dimension of the generated PRV is p , i.e. the PRV has p independent elements. To get a non-trivial solution to the PRV, at least, $p \geq 1$ must be guaranteed. Further, if one still uses the isolation logic given in Table 1 to design a set of SRVs, each SRV will have $p - s$ independent elements. Therefore, to ensure the isolation of single actuator fault at one time, $p - s \geq 1$ should always hold. Finally, under the constraint $p - s \geq 1$, a larger n_0 is preferred. As a consequence, more components in the uncertainty vector $\mathbf{e}_{s-1,k-1}^*$ will be removed from the PRV.

4.3.2. Condition for fault detectability

It follows from Eq. (21) that the mean of $\mathbf{e}_{s,k}$ in the presence of actuator faults is

$$\begin{aligned} E\{\mathbf{e}_{s,k}\} &= \{\mathbf{W}_\circ \mathbf{H}_s^\circ + \mathbf{M}(\mathbf{I}_s \otimes \delta \mathbf{B})\} E\{\mathbf{f}_{s-1,k-1}^u\} \\ &\quad + \mathbf{M} \mathbf{e}_{s-1,k-1}^*. \end{aligned} \quad (22)$$

In this case, the fault detection index $\eta_{s,k}$ is a non-central chi-square distributed random variable with non-centrality parameter $\|\mathbf{M} \mathbf{e}_{s-1,k-1}^* + [\mathbf{M}(\mathbf{I}_s \otimes \delta \mathbf{B}) + \mathbf{W}_\circ \mathbf{H}_s^\circ] E\{\mathbf{f}_{s-1,k-1}^u\}\|^2$.

$\{\mathbf{f}_{s-1,k-1}^u\}^2$. To ensure the detectability of any actuator faults, $\|\mathbf{M}\mathbf{e}_{s-1,k-1}^* + [\mathbf{M}(\mathbf{I}_s \otimes \delta\mathbf{B}) + \mathbf{W}_o\mathbf{H}_s^o]E\{\mathbf{f}_{s-1,k-1}^u\}\|^2 \geq s^2L_m^2\lambda_{max}^M$ must hold.

To simplify the above detectability condition, denote

$$FDR_k = \frac{\|[\mathbf{M}(\mathbf{I}_s \otimes \delta\mathbf{B}) + \mathbf{W}_o\mathbf{H}_s^o]E\{\mathbf{f}_{s-1,k-1}^u\} + \mathbf{M}\mathbf{e}_{s-1,k-1}^*\|}{\|\mathbf{M}\mathbf{e}_{s-1,k-1}^*\|},$$

$$BDR_k = \frac{sL_m\sqrt{\lambda_{max}^M}}{\|\mathbf{M}\mathbf{e}_{s-1,k-1}^*\|},$$

where FDR_k and BDR_k stand for fault-to-disturbance ratio and boundary-to-disturbance ratio at time instant k , respectively. Thus, the detectability condition can be rewritten as $FDR \geq BDR$. Therefore, if the FDI system has been designed, i.e. the matrices \mathbf{M} and \mathbf{W}_o are fixed, the detectability condition of actuator faults depends on the relationship between the fault-to-disturbance ratio and the boundary-to-disturbance ratio.

5. Numerical example and experimental case study

In this section, a numerical example and a real experimental case study are provided to demonstrate the validity of the proposed robust FDI scheme. A numerical example is simulated first, which includes FDI of sensors and actuators faults.

5.1. Numerical example

5.1.1. The simulated CSTR process

Consider a simulated non-isothermal continuous stirred tank reactor (CSTR) process (Marlin, 1995, pp. 90–92), as depicted in Fig. 2. The process has one feed stream, which is merged from the solvent and the reactant, one product stream, and a coolant flowing through the coil. The flows of the reactant (F_A) and the coolant (F_C) are used to control the residual concentration (C_A) and the outlet temperature (T), respectively. In

addition, the reactant concentration in the solvent feed (C_{AS}) and the inlet temperature (T_o) are simulated as unmeasured disturbances.

The simulation parameters and initial conditions are selected to be the same as in Yoon and MacGregor (2001). Note that variables in the CSTR process, e.g. T and C_A , are functions of time. The argument of the process variables is omitted for simplicity.

After being linearized around a steady operating point, the simulated CSTR process is represented by a second-order continuous-time state space model with two inputs, four outputs and two unmeasured disturbances. In the model, the state variables are $\mathbf{x}_t = [C_A \ T]^t$; the inputs are $\mathbf{u}_t = [F_C \ F_A]^t$; and the disturbances are $\mathbf{d}_t = [C_{AS} \ T_o]^t$. The temperature T and the residual concentration C_A are controlled by two proportional controllers with unit gains.

After discretizing the continuous-time system model using a sampling period $T_s = 0.5$ min, the following discrete-time state space model is obtained:

$$\begin{aligned} \mathbf{x}_{k+1} &= \mathbf{A}\mathbf{x}_k + \mathbf{B}\mathbf{u}_k + \mathbf{E}\mathbf{d}_k, \\ \mathbf{y}_k &= \mathbf{C}\mathbf{x}_k + \mathbf{o}_k, \end{aligned} \tag{23}$$

where

$$\mathbf{A} = \begin{bmatrix} 0.2828 & -0.0005939 \\ 1.258 & 0.04251 \end{bmatrix},$$

$$\mathbf{B} = \begin{bmatrix} 0.0002216 & 0.5398 \\ -0.1042 & 1.576 \end{bmatrix},$$

$$\mathbf{C} = \begin{bmatrix} 1 & 0 & 1 & 0 \\ 0 & 1 & 0 & 1 \end{bmatrix}', \quad \mathbf{E} = \begin{bmatrix} 0.2844 & -0.00032506 \\ 0.68872 & 0.15287 \end{bmatrix}.$$

In addition, \mathbf{x}_k , \mathbf{u}_k and \mathbf{d}_k are sampled values of \mathbf{x}_t , \mathbf{u}_t and \mathbf{d}_t at $t = kT_s$, respectively; and \mathbf{o}_k is a Gaussian distributed white noise vector with covariance $diag([2.5 \times 10^{-5}, 4 \times 10^{-4}, 2.5 \times 10^{-5}, 4 \times 10^{-4}])$.

Note that in the preceding equation, there are four outputs (two sensors for C_A and T , and two additional

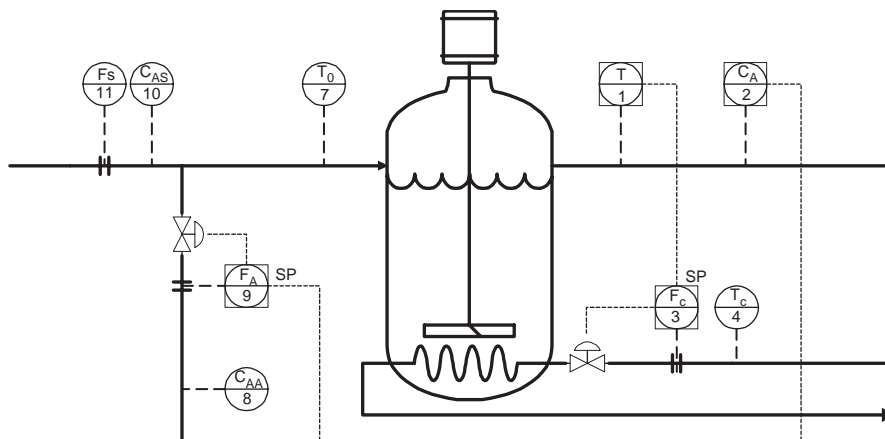


Fig. 2. Process schematic of the simulated nonisothermal CSTR system.

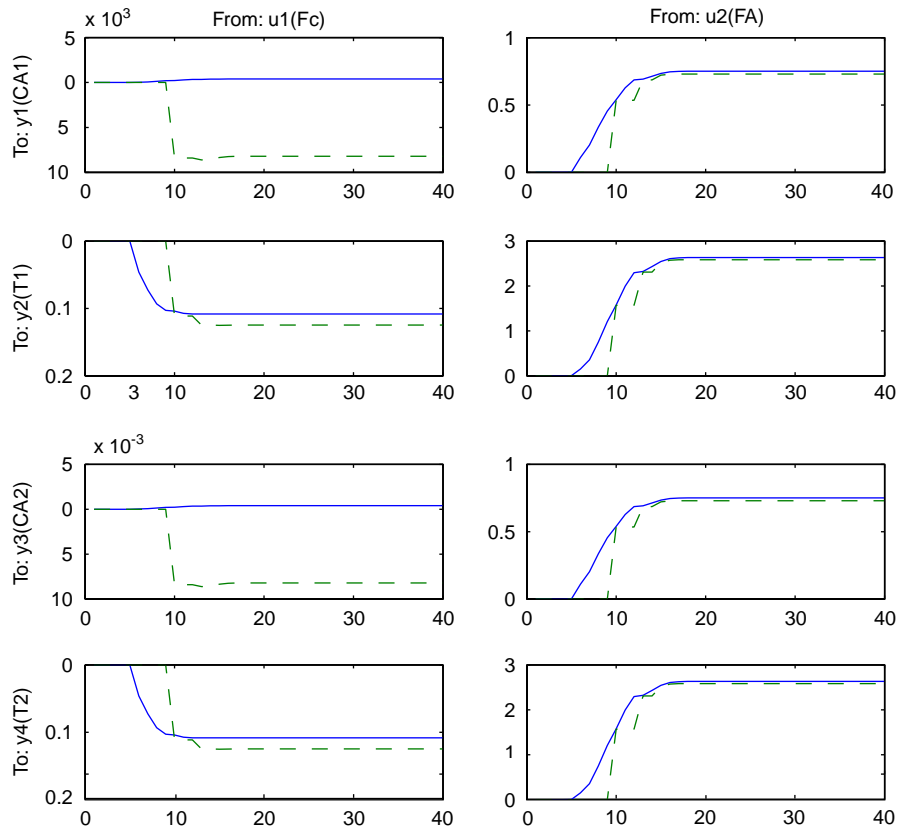


Fig. 3. Step responses from the true model and its identified model of the simulated CSTR process (solid line: real system step response; dashed line: model step response).

sensors are introduced to satisfy the condition for perfect uncertainty decoupling).

Four hundred samples of training data were collected to identify the system matrices by means of the *N4SID* function in *Matlab*[®], and obtain one estimate of \mathbf{A} , \mathbf{B} and \mathbf{C} as follows:

$$\mathbf{A}_o = \begin{bmatrix} 0.35548 & -0.025014 \\ 1.3213 & 0.020207 \end{bmatrix},$$

$$\mathbf{B}_o = \begin{bmatrix} -0.0084123 & 0.53482 \\ -0.11132 & 1.5683 \end{bmatrix}, \quad \mathbf{C}_o = \mathbf{C}.$$

Notice that \mathbf{A}_o and \mathbf{B}_o are apparently biased from their true values. For example, look at the step response of the real system (solid line) and the estimated system (dashed line) shown in Fig. 3, they are different due to the MPM. As will be seen later, the presence of MPM may make the conventional Chow–Willsky method unworkable.

5.1.2. Sensor FDI for the CSTR

Using \mathbf{A}_o , \mathbf{B}_o and \mathbf{C}_o , construct $\Psi_s^o \in \mathcal{R}^{12 \times 6}$ and $\mathbf{H}_s^o \in \mathcal{R}^{12 \times 4}$. Subsequently, $\mathbf{W}_o \in \mathcal{R}^{6 \times 12}$ is calculated according to Eq. (8), obtaining the PRV model $\mathbf{W}_o[\mathbf{I}_{m_s} | -\mathbf{H}_s^o] \in \mathcal{R}^{6 \times 16}$. Further, based on the isolation logic shown in Table 1 ($m = 4$), four transformation

matrices: $\mathbf{W}_i \in \mathcal{R}^{3 \times 6}$, $\forall i = [1, 4]$ are calculated to generate four SRVs, respectively, for fault isolation.

Using the calculated PRV model and the same training data, a sequence of PRV is produced, from which the covariance matrices $\mathbf{R}_{s,e} \in \mathcal{R}^{6 \times 6}$ and $\mathbf{R}_{s,e}^i = \mathbf{W}_i \mathbf{R}_{s,e} \mathbf{W}_i' \in \mathcal{R}^{3 \times 3}$, $\forall i = [1, 4]$, are estimated. Since the PRV is six-dimensional, the fault detection index $\eta_{s,k} = \mathbf{e}_{s,k}' \mathbf{R}_{s,e}^{-1} \mathbf{e}_{s,k}$ in the fault-free case is a chi-square random variable with 6 degrees of freedom, i.e. $\eta_{s,k} \sim \chi^2(6)$. Given a level of significance, e.g. $\alpha = 0.01$, the confidence limit for $\eta_{s,k}$ is $\chi_{0.01}^2(6) = 16.812$. Moreover, four fault isolation indices $\eta_{s,k}^i$, $\forall i = [1, 4]$ are computed. With the same α , their confidence limits are $\chi_{0.01}^2(3) = 11.341$.

Four types of faults (Qin & Li, 1999), e.g. bias, drift, complete failure, and precision degradation, are simulated in this example. Due to the lack of space, only results for detection and isolation of a bias type fault is presented in this paper.

A bias $f_{k,i} = 0.05$ is introduced to one of the four sensors from 500 to 700 sample instants. From the test data, $\eta_{s,k}$ for fault detection and $\eta_{s,k}^i$, $\forall i = [1, 4]$, for fault isolation are calculated. For better visualization, $\eta_{s,k}$ and $\eta_{s,k}^i$, $\forall i = [1, 4]$, have been scaled by their respective confidence limits, e.g. $\bar{\eta}_{s,k} = \eta_{s,k} / \chi_{0.01}^2(6)$ and $\bar{\eta}_{s,k}^i = \eta_{s,k}^i / \chi_{0.01}^2(3)$. As a result, $\bar{\eta}_{s,k}$ and $\bar{\eta}_{s,k}^i$ have a common unit confidence limit.

The FDI results are presented in Fig. 4, where FD stands for $\bar{\eta}_{s,k}$ and $FI_i, \forall i = [1, 4]$ for $\bar{\eta}_{s,k}^i$, respectively. As can be seen clearly in the figure, a fault is detected at $k = 500$. In addition, the first fault isolation index $\bar{\eta}_{s,k}^1$ is within the confidence limit all the time, while the other isolation indices $\bar{\eta}_{s,k}^i, \forall i = [2, 4]$, are all beyond the limit after the occurrence of the fault. This produces an incidence code [0 1 1 1], from which one can correctly infer that the first output sensor is faulty.

In order to demonstrate the advantage of the proposed robust FDI method, a comparison with the original Chow–Willsky scheme (Chow & Willsky, 1984) is carried out. The Chow–Willsky approach-based FDI results using the same test data and the same estimated state space model are given in Fig. 5. In the figure, the fault detection index and some of the fault isolation indices are outside their respective thresholds even after the fault has disappeared due to the effect of process uncertainties. For instance, the first fault isolation index $\bar{\eta}_{s,k}^1$ is beyond the limit, producing an incidence code [1 1 1 1], which is different from the pre-determined incidence code [0 1 1 1]; hence the fault is not isolated correctly.

5.1.3. Actuator FDI for the CSTR

Using this numerical example, actuator FDI is also carried out. First, a PRV is designed which is insensitive to the first left singular vector of \mathbf{G}_s° i.e. $n_0 = 1$. The singular values of \mathbf{G}_s° are displayed in Table 2, where the first singular value accounts for 42.86% of the total variance of the process uncertainty vector $\mathbf{e}_{s-1,k-1}^*$. Therefore, 42.86% of the process uncertainties has been

removed from the PRV. The dimension of the PRV in this case is 9. Choose L_m to be equal to $3 \max(\|\mathbf{B}_o \mathbf{u}_k^*\|) = 0.363$. Consequently, the fault detection index is a non-central chi-square random variable with degrees of freedom 3 and non-centrality parameter 0.6756. With $\alpha = 0.01$, the confidence limit for the fault detection index is 13.6104. Further, from the PRV, two SRVs are generated for actuator fault isolation, which are made insensitive to fault in the first and second actuators, respectively. Similarly, we can define two fault isolation indices: $\{\eta_{s,k}^1, \eta_{s,k}^2\}$, which are associated with the SRVs.

A bias fault $f_{k,i} = 1.3$ is introduced to one of two actuators. The FDI results are displayed in Fig. 6, where the FDI indices have also been scaled to have unit confidence limit. As clearly shown in the figure, fault detection is successfully done, because the detection index is beyond its confidence limit after the occurrence of fault. Moreover, since the first isolation index is within its confidence limit, while the second isolation index is beyond its confidence limit, it can be concluded that the first actuator has a fault according to the pre-determined isolation logic. Note that in the figure, FD stands for the scaled fault detection index, and $FI_j, j = 1, 2$, stand for the scaled fault isolation indices.

Since the state and the disturbance vectors are known in this simulation example, the validity of the detectability condition for actuator faults can be checked. In this simulation example, the maximum boundary-to-disturbance ratio is 13.7441. On the other side, $FDR_k = 13.8062$. Therefore, it verifies that the detectability condition of actuator faults is satisfied.

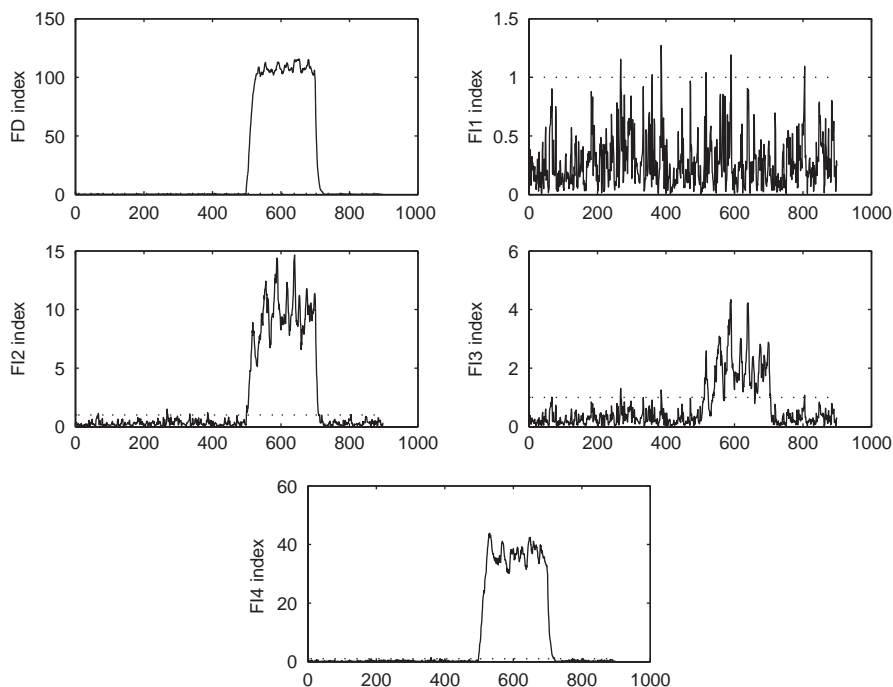


Fig. 4. Detection and isolation of a bias fault in the first output sensor of the simulated CSTR process using the proposed robust FDI scheme.

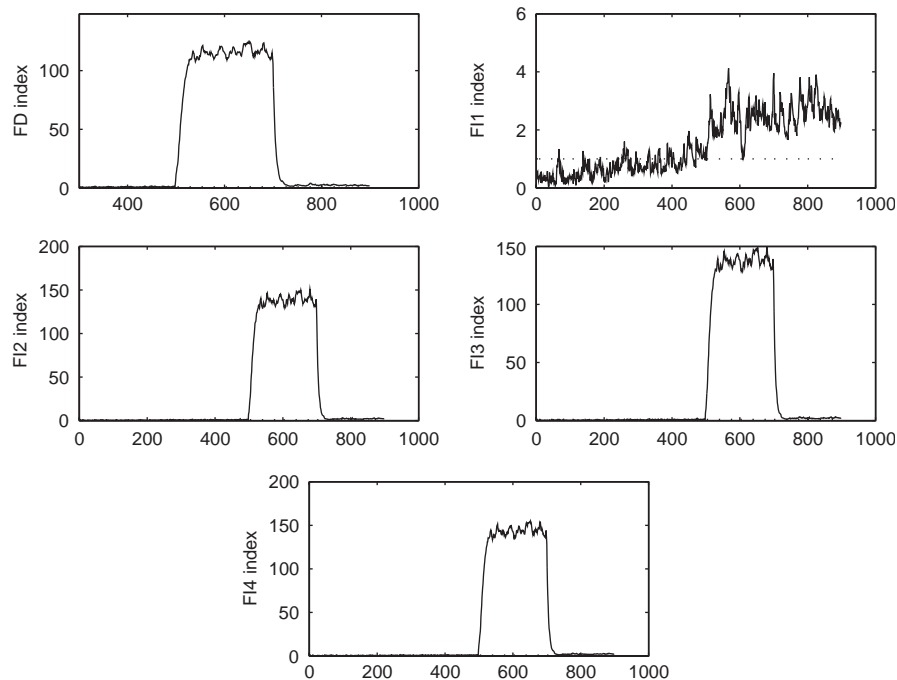


Fig. 5. Detection and isolation results of a bias fault in the first output sensor of the simulated CSTR process using the Chow–Willsky approach.

Table 2
Singular values of matrix G_s° and their cumulative percentages

| No. | Singular values | Cumulative percentages |
|-----|-----------------|------------------------|
| 1 | 2.6811 | 42.86% |
| 2 | 1.4352 | 65.80% |
| 3 | 1.3936 | 88.08% |
| 4 | 0.7460 | 100% |

5.2. Experimental case study

In this experimental case study, a real continuous stirred tank heater (CSTH) is used for sensor FDI. The CSTH system is located in the Computer Process Control Laboratory, Department of Chemical and Materials Engineering, University of Alberta, Canada.

The CSTH system has two inputs: cold water (CW) and steam (S); four measured outputs: cold water flow rate (F_C), water level (L), and two outlet water temperatures (T_1 and T_2); and one major disturbance: hot water (HW). The cold water and hot water are well mixed in the tank and heated at the same time by the high pressure steam passing through a coil. The water level is controlled by cold water valve using a PID controller. Two outlet water temperature sensors are located at different locations on a long outlet pipeline. Even though both sensors measure the same physical variable, their readings are not identical due to the different time delays and heat losses. The inputs and outputs vectors are $\mathbf{u} = [CW \ S]^T$ and $\mathbf{y} = [L \ F_C \ T_1 \ T_2]^T$, respectively, and they are sampled every 5 seconds

during this study. The overall system block diagram is shown in Fig. 7.

From this pilot plant, a set of training data with 400 points is first collected. Subsequently, a second-order discrete-time state space model is identified by using the *N4SID* function in *Matlab*[®], where

$$\mathbf{A}_o = \begin{bmatrix} 0 & 1 \\ -0.7494 & 1.6504 \end{bmatrix},$$

$$\mathbf{B}_o = \begin{bmatrix} -0.1652 & -0.0011 \\ -0.2727 & 0.0029 \end{bmatrix},$$

$$\mathbf{C}_o = \begin{bmatrix} -1.1527 & 1.5935 \\ 0.6940 & -3.8102 \\ 1.0125 & -0.0086 \\ 1 & 0 \end{bmatrix}.$$

Selecting $s = n = 2$ and using the same procedure as in the preceding numerical example, a PRV for fault detection and four SRVs for fault isolation can be generated, where the isolation logic in Table 1 is still used.

A bias type of fault $f_{k,i} = 1.0$ is introduced to a sensor between the 100th to 200th sampling instants. Fig. 8 illustrates the relevant FDI result, where the fault detection index and fault isolation indices are also scaled to have unit confident limit. In the figure, the fault is detected immediately after it occurs. In addition, it can be inferred that the 3rd output, i.e. the first temperature sensor, is faulty, because the fault isolation indices have an incidence code [1 1 0 1].

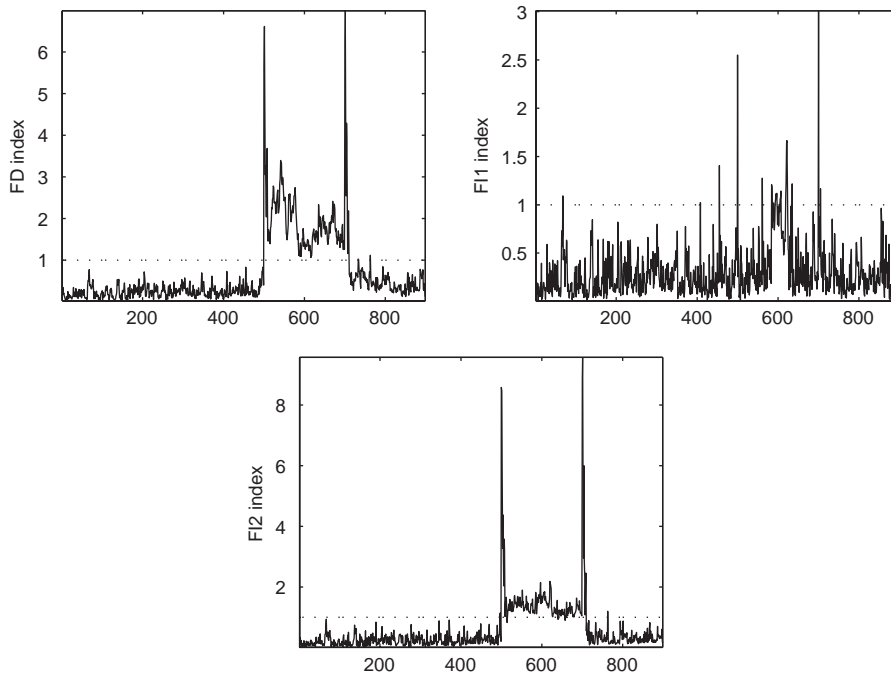


Fig. 6. Detection and isolation results of a bias fault in the first actuator of the simulated CSTR process using the proposed robust FDI approach.

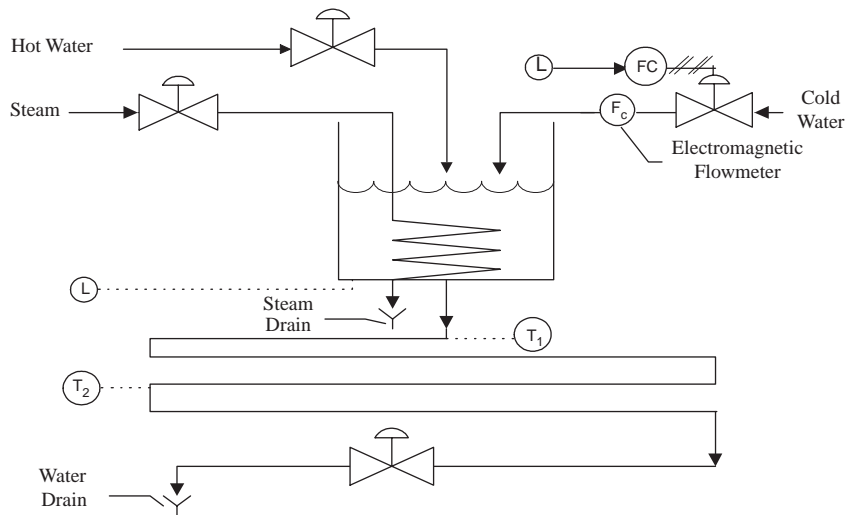


Fig. 7. Process schematic of the experimental CSTR system.

The Chow–Willsky approach is also applied to the same case study. The corresponding FDI result is shown in Fig. 9, where the fault is not correctly detected and isolated, due to the presence of the process uncertainties.

6. Conclusions

A robust scheme for the detection and isolation of sensor/actuator faults in dynamic processes has been proposed in this paper. In the presence of sensor faults,

this approach can perfectly decouple the effect of any process uncertainties, including MPM and unmeasured disturbances from the PRV, if the number of process uncertainties is less than the number of outputs. In the presence of actuator faults, the principal components of the process uncertainties can be removed from the PRV. Therefore, robust actuator FDI can be also achieved.

This newly proposed method is applied to a simulated CSTR system and an experimental pilot scale plant, respectively. In both cases, satisfactory FDI results are

obtained. In addition, in both cases comparisons between the newly proposed FDI method with the Chow–Willsky approach have been made. It is demonstrated that the newly proposed FDI approach has acceptable robustness with respect to process uncertainties and high sensitivity to faults.

Acknowledgements

The project has been financially supported by the Natural Sciences and Engineering Research Council (NSERC), Matrikon Inc. (Edmonton, Alberta), and the Alberta Science and Research Authority (ASRA), of

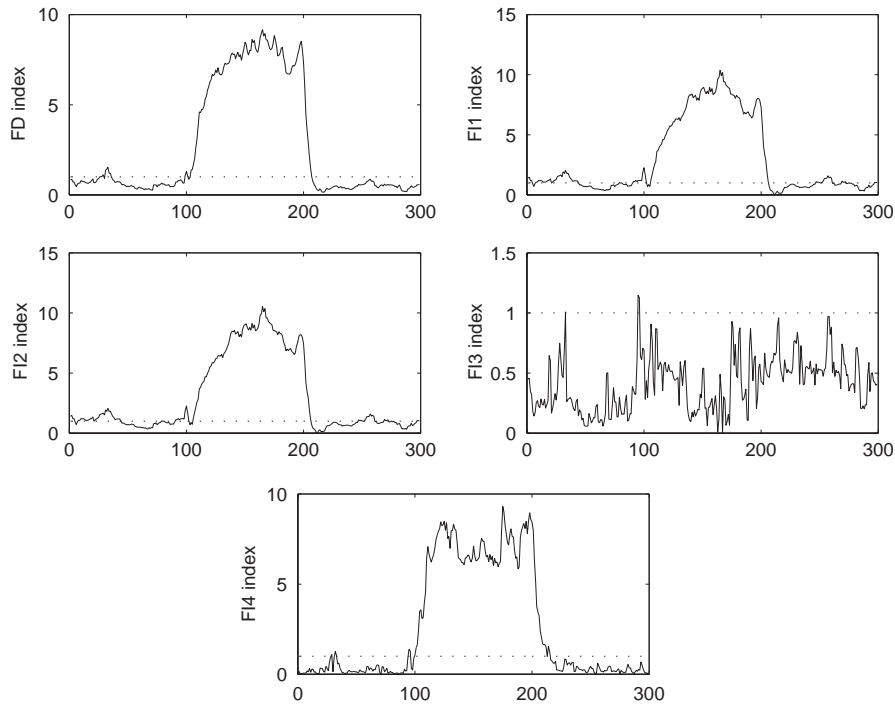


Fig. 8. Detection and isolation of a bias fault in the third output sensor of the experimental CSH system using the proposed robust FDI approach.

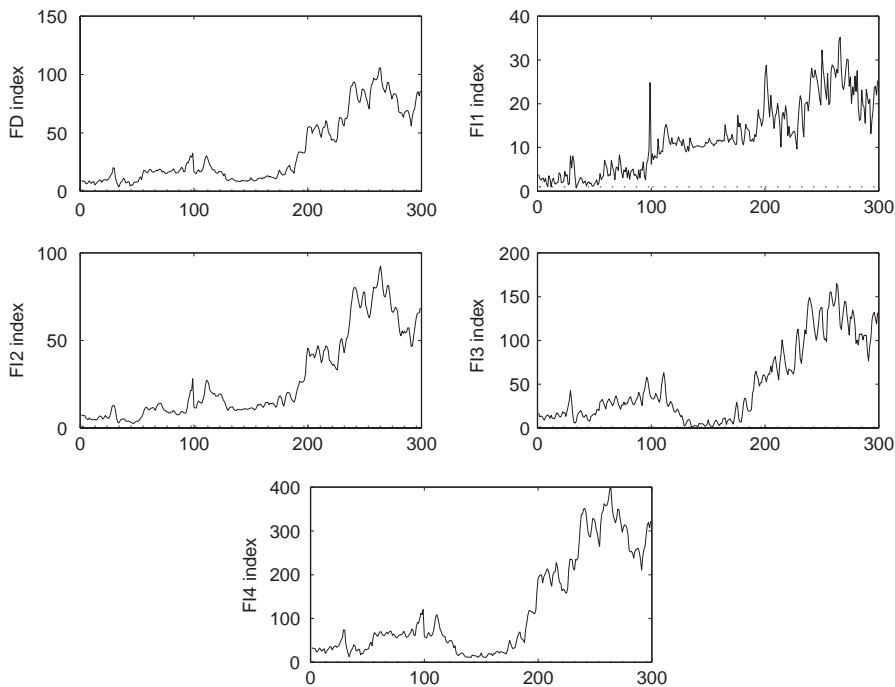


Fig. 9. Detection and isolation results of a bias fault in the third output sensor of the experimental CSH system using the Chow–Willsky approach.

Canada, through the NSERC-Matrikon-ASRA Senior Industrial Research Chair program at the University of Alberta. The authors would also like to acknowledge the constructive comments given by the anonymous reviewers.

References

- Basseville, M. (1998). On-board component fault detection and isolation using the statistical local approach. *Automatica*, *34*, 1391–1415.
- Basseville, M., & Nikiforov, I. (1993). *Detection of abrupt changes—theory and applications*. Englewood Cliffs, NJ: Prentice-Hall.
- Chen, J., & Patton, R. (1999). *Robust Model-based fault diagnosis for dynamic systems*. Dordrecht: Kluwer Academic Publisher.
- Chen, J., Patton, R., & Zhang, H. (1996). Design of unknown input observers and robust fault detection filters. *International Journal of Control*, *63*, 85–105.
- Chow, E., & Willsky, A. (1984). Analytical redundancy and the design of robust failure detection systems. *IEEE Transactions on Automatic Control*, *29*, 603–614.
- Frank, P. (1990). Fault diagnosis in dynamic systems using analytical and knowledge-based redundancy—a survey and some new results. *Automatica*, *26*, 459–474.
- Frank, P. (1994). Enhancement of robustness in observer-based fault detection. *International Journal of Control*, *59*, 955–981.
- Frank, P., & Ding, X. (1994). Frequency domain approach to optimally robust residual generation and evaluation for model-based fault diagnosis. *Automatica*, *30*, 789–804.
- Frank, P., & Ding, X. (1997). Survey of robust residual generation and evaluation methods in observer-based fault detection systems. *Journal of Process Control*, *7*, 403–424.
- Gertler, J. (1988). Survey of model-based failure detection and isolation in complex plants. *IEEE Control System Magazine*, *12*, 3–11.
- Gertler, J. (1991). Analytical redundancy method in fault detection and isolation, survey and synthesis. In *Proceedings of the IFAC SAFEPROCESS symposium*, 10–13 September 1991.
- Gertler, J. (1998). *Fault detection and diagnosis in engineering systems*. New York: Marcel Dekker.
- Gertler, J., & Kunwer, M. (1995). Optimal residual decoupling for robust fault diagnosis. *International Journal of Control*, *61*, 395–421.
- Gertler, J., & Singer, D. (1985). Augmented models for statistical fault isolation in complex dynamic systems. In *Proceedings of the American Control Conference* (pp. 317–322).
- Gertler, J., & Singer, D. (1990). A new structural framework for parity equation based failure detection and isolation. *Automatica*, *26*, 381–388.
- Golub, G., & Van Loan, C. (1996). *Matrix computations* (3rd ed.). Baltimore: The Johns Hopkins University Press.
- Gustafsson, F., & Graebe, S. (1998). Closed-loop performance monitoring in the presence of system changes and disturbances. *Automatica*, *34*, 1311–1326.
- Hamelin, F., & Sauter, D. (2000). Robust fault detection in uncertain dynamic systems. *Automatica*, *36*, 1747–1754.
- Isermann, R. (1984). Process fault detection based on modeling and estimation methods—a survey. *Automatica*, *20*, 387–404.
- Johnson, R., & Wichern, D. (1998). *Applied multivariate statistical analysis* (4th ed.). Englewood Cliffs, NJ: Prentice-Hall.
- Li, W., & Shah, S. (2002). Structured residual vector-based approach to sensor fault detection and isolation. *Journal of Process Control*, *12*, 429–443.
- Lou, X., Willsky, A., & Verghese, G. (1986). Optimally robust redundancy relations for failure detection in uncertain systems. *Automatica*, *22*, 333–344.
- Marlin, T. (1995). *Process control—designing processes and control systems for dynamic performance*. New York: McGraw-Hill.
- Patton, R., & Chen, J. (1992). Robust fault detection of jet engine sensor systems using eigenstructure assignment. *Journal of Guidance, Control and Dynamics*, *15*, 1491–1497.
- Patton, R., & Chen, J. (2000). On eigenstructure assignment for robust fault diagnosis. *International Journal of Robust and Nonlinear Control*, *10*, 1193–1208.
- Patton, R., Frank, P., & Clark, R. (1989). *Fault diagnosis in dynamic systems*. Englewood Cliffs, NJ: Prentice Hall.
- Patton, R., Frank, P., & Clark, R. (Eds.). (2000). *Issues of fault diagnosis for dynamic systems*. Berlin: Springer.
- Proakis, J. (1989). *Digital Communications* (2nd ed.). McGraw-Hill Book Company.
- Qin, S., & Li, W. (1999). Detection, identification, and reconstruction of faulty sensors with maximized sensitivity. *A.I.Ch.E. Journal*, *45*, 1963–1976.
- Qin, S., & Li, W. (2001). Detection and identification of faulty sensors in dynamic processes. *A.I.Ch.E. Journal*, *47*, 1581–1593.
- Shen, L., & Hsu, P. (1998). Robust design of fault isolation observers. *Automatica*, *34*, 1421–1429.
- Willsky, A. (1976). A survey of design methods for failure detection in dynamic systems. *Automatica*, *12*, 601–611.
- Yoon, S., & MacGregor, J. (2001). Fault diagnosis with multivariate statistical models part I: using steady state fault signatures. *Journal of Process Control*, *11*, 387–400.
- Zhong, M., Ding, S., Lam, J., & Wang, H. (2003). An LMI approach to design robust fault detection filter for uncertain LTI systems. *Automatica*, *39*, 543–550.